Hadron mass spectrum and the shear viscosity to entropy density ratio of hot hadronic matter

Jacquelyn Noronha-Hostler and Jorge Noronha
Instituto de Física, Universidade de São Paulo, C.P. 66318, 05315-970 São Paulo, São Paulo, Brazil

Carsten Greiner
Institut für Theoretische Physik, Goethe Universität, Frankfurt, Germany
(Received 1 July 2012; published 27 August 2012)

Lattice calculations of the QCD trace anomaly at temperatures $T < 160$ MeV have been shown to match hadron resonance gas model calculations, which include an exponentially rising hadron mass spectrum. In this paper we perform a more detailed comparison of the model calculations to lattice data that confirms the need for an exponentially increasing density of hadronic states. Also, we find that the lattice data is compatible with a hadron density of states that goes as $\rho(m) \sim m^{-a} \exp(m/T_H)$ at large m with $a > 5/2$ (where $T_H \sim 167$ MeV). With this specific subleading contribution to the density of states, heavy resonances are most likely to undergo two-body decay (instead of multiparticle decay), which facilitates their inclusion into hadron transport codes. Moreover, estimates for the shear viscosity and the shear relaxation time coefficient of the hadron resonance model computed within the excluded volume approximation suggest that these transport coefficients are sensitive to the parameters that define the hadron mass spectrum.

DOI: 10.1103/PhysRevC.86.024913 PACS number(s): 12.38.Mh, 24.10.Pa, 24.85.+p, 25.75.Dw

I. INTRODUCTION

Particle flow anisotropies at low transverse momentum produced in ultrarelativistic heavy-ion collisions can be reasonably described [1–3] using relativistic fluid dynamics with a very small shear viscosity to entropy ratio $\eta/s \sim 1/(4\pi)$. This is as small as the uncertainty principle-based estimate derived by Danielewicz and Gyulassy nearly 30 years ago [4] and also the more recent calculations [5] performed in strongly coupled gauge theories dual to higher dimensional theories of gravity [6]. Beyond-leading log perturbative QCD calculations that are applicable at temperatures $T > m_{\rm pion}$ give values for the ratio that are an order of magnitude larger than the bound [7] (for calculations based on parton transport, see Ref. [8]). Moreover, calculations performed using hadronic models at $T \sim m_{\rm pion}$ also resulted in values for the ratio above the viscosity bound [9–12].

Owing to the observation made in Ref. [13] that a small value of η/s in QCD should occur in the transition region $T \sim 150$–200 MeV owing to the rapid increase in the entropy density observed in lattice simulations [14,15], the effects of an exponentially increasing density of hadronic states on several properties of hot hadronic matter were investigated using the hadron resonance gas model in Refs. [16–20]. It was shown in those studies that the addition of new hadronic states that follow an exponentially increasing hadron mass spectrum as proposed by Hagedorn [21],

$$\lim_{m\to\infty} \rho(m) \sim \frac{e^{m/T_H}}{m^{5/2}}, \tag{1}$$

to the hadron resonance gas model led to a much better agreement to the lattice data computed around the pseudocritical QCD critical temperature $T_c \sim 196$ MeV inferred from Ref. [22]. Moreover, an estimate of η/s at $T \sim 190$ MeV computed using this model indicated that excited hadronic matter at those temperatures could become a nearly perfect fluid [23] where η/s approached $1/(4\pi)$. In this case, the transition from viscous hydrodynamics to typical hadronic transport would be much smoother than expected. However, with the advent of the lattice calculations published in Ref. [15] and the smaller critical region $T \sim 155$ MeV [24] obtained in those studies (which has been independently confirmed in [25]), a revision of the effects of heavy resonances on the hadron resonance gas model became necessary. Reference [26] showed that a hadron resonance gas model containing only the known hadrons and resonances could only describe the lattice data up to $T \sim 140$ MeV, while the inclusion of states with mass $m > 2$ GeV (which follow an exponential spectrum) could improve the match to the lattice data of Ref. [15] and provide a good description of lattice QCD thermodynamics up to $T = 155$ MeV.

In this paper we present a more detailed comparison between the hadron resonance gas model calculations and the lattice data that not only provides strong evidence for the need of an exponentially increasing density of hadronic states with mass $m > 2$ GeV but also indicates that the density of states goes as $\rho(m) \sim m^{-a} \exp(m/T_H)/$ at large m with $a > 5/2$ (where $T_H \sim 167$ MeV). As in Ref. [26], we estimate that the maximum temperature at which the hadron resonance gas model is applicable is $\sim$155 MeV. A rough estimate of the shear viscosity computed within the excluded volume approximation for the hadron resonance model suggests that the shear viscosity to entropy ratio of hot hadronic matter is sensitive to the parameters that describe the hadron mass spectrum. We briefly comment also on the value of the shear relaxation time coefficient of hot hadronic matter.

II. HADRON MASS SPECTRUM AND THE HADRON RESONANCE GAS MODEL

In the statistical bootstrap model of hadrons [21,27], a hadron is considered to be a volume V (with typical length $\sim$1 fm) composed of two or more freely roaming constituents and the hadron density of states is required to be consistent with the spectrum of constituents, which are themselves hadrons.

This is the so-called "bootstrap condition" pioneered in this context by Hagedorn in 1965 [21]. Frautschi [27] reformulated the bootstrap condition and wrote down an equation for the total density of states $\rho(m)$ in the hadronic volume (for Boltzmann statistics) where different states of mass m_i and energy $E_i = \sqrt{p_i^2 + m_i^2}$ inside the box possess single particle density $\rho_{in}(m_i)$. The bootstrap condition

$$\lim_{m\to\infty} \rho(m) \Longrightarrow \rho_{in}(m) \tag{2}$$

is exactly satisfied when $\lim_{m\to\infty} \rho(m) \sim c\, e^{bm}/m^a$ with $a > 5/2$ [27]. This exponentially rising mass spectrum is typical of a system consisting of stringlike constituents such as a gas of free strings [28–30] or large N_c glueballs [31]. The spectrum of experimentally measured hadrons [32] was found to be compatible with an exponential increase of the number of states up to ∼1.7 GeV [33,34], although the subleading power a cannot be reliably determined from such an analysis.

Once the hadron mass spectrum is given, the thermodynamical quantities of the hadron resonance gas model (at zero chemical potential) in the total volume V and temperature T are fully determined by the partition function (assuming Boltzmann statistics),

$$Z(T, V) = \sum_{N=0}^{\infty} \frac{1}{N!} \prod_{i=1}^{N} \int dm_i\, \rho(m_i) \int \frac{d^3 p_i}{(2\pi)^3} e^{-E_i/T} V^N, \tag{3}$$

which can be used to determine the usual thermodynamic functions. In fact, one finds

$$p(T) = \frac{T^2}{2\pi^2} \int_0^{\infty} dm\, \rho(m) m^2 K_2\left(\frac{m}{T}\right) \tag{4}$$

for the pressure,

$$\varepsilon(T) = \frac{1}{2\pi^2} \int_0^{\infty} dm\, \rho(m) m^4 \times \left[3\left(\frac{T}{m}\right)^2 K_2\left(\frac{m}{T}\right) + \left(\frac{T}{m}\right) K_1\left(\frac{m}{T}\right)\right] \tag{5}$$

for the energy density,

$$s(T) = \frac{dp(T)}{dT} = \frac{1}{2\pi^2} \int_0^{\infty} dm\, \rho(m) m^3 K_3\left(\frac{m}{T}\right) \tag{6}$$

for the entropy density, and

$$\varepsilon(T) - 3p(T) = \frac{T}{2\pi^2} \int_0^{\infty} dm\, \rho(m) m^3 K_1\left(\frac{m}{T}\right) \tag{7}$$

for the trace anomaly. The speed of sound can be found from the relation $c_s^2 = dp/d\varepsilon$. In this paper we discuss four different forms for the density of states,

$$\rho_1(m) = A_1\, e^{m/T_{H_1}}, \tag{8}$$

$$\rho_2(m) = \frac{A_2}{\left[m^2 + m_{02}^2\right]^{5/4}} e^{m/T_{H_2}}, \tag{9}$$

$$\rho_3(m) = \frac{A_3}{\left[m^2 + m_{03}^2\right]^{3/2}} e^{m/T_{H_3}}, \tag{10}$$

$$\rho_4(m) = \frac{A_4}{T_{H_4}} \left(\frac{m}{T_{H_4}}\right)^{\alpha}, \tag{11}$$

where the parameters are shown in Table I.

TABLE I. Parameters for the mass spectra shown in Eqs. (8)–(11).

	T_H (GeV)	A	m_0 (GeV)	α
ρ_1	0.252	2.84 (1/GeV)		
ρ_2	0.180	0.63 (GeV$^{3/2}$)	0.5	
ρ_3	0.175	0.37 (GeV^2)	0.5	
ρ_4	0.158	0.51		2

The parameters chosen for ρ_1 and ρ_2 are the same ones used in Ref. [26] while the parameters for the other ρ's were obtained from a fit to the lattice data of Ref. [15]. The density ρ_3 satisfies the asymptotic bootstrap condition exactly, while ρ_1 (introduced in Ref. [26]) and Hagedorn's ρ_2 satisfy the bootstrap condition within a power of m [27]. The power law increase given by ρ_4 (introduced by Shuryak in the early 1970s [35]) does not satisfy the bootstrap condition (it also does not lead to any singularities in the thermodynamics), but it provides a nice alternative to describe the rise of the hadronic mass spectrum. As discussed in Ref. [26], the trace anomaly at temperatures around 160 MeV becomes sensitive to the heavy states in the spectrum with mass $m > 2$ GeV. A comparison between the different ρ's used here can be found in Fig. 1, where the integrand (in units of 1/GeV) in Eq. (7) is plotted as a function of m at $T = 150$ MeV. One can see that the integrand computed using the first three ρ's (black solid, blue dashed, and red long-dashed curves, respectively) are very similar but they can be clearly distinguished from the result obtained using the power law in ρ_4 (small-dashed green curve).

Even though the upper limit of the mass integrals in Eqs. (4)–(7) is taken to be infinity, the divergences implied by an exponentially rising spectrum do not appear in the calculations performed here because the limiting temperatures T_{H_i}'s ($i = 1, 2, 3$) are above the largest temperature considered in this paper, ∼160 MeV. One may wonder if the

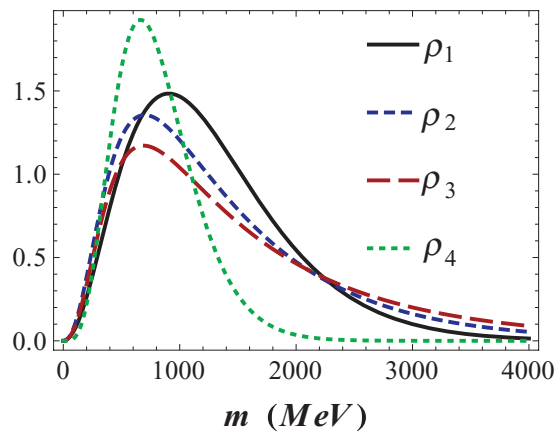

FIG. 1. (Color online) Comparison between the integrand (in units of 1/GeV) in Eq. (7) computed using the different ρ's at $T = 150$ MeV as a function of m. The black line was computed using ρ_1, the blue dashed line with ρ_2, the red long-dashed line with ρ_3, while the short-dashed green line was obtained using ρ_4.

approximations made in Eqs. (4)–(7) (i.e., classical statistics and continuous mass spectrum) are at all justified. After all, we know that the measured hadronic spectrum is, of course, discrete and that baryons and mesons obey different statistics. However, as pointed out in Ref. [26], the simplified formulas in Eqs. (4)–(7) provide an excellent description of the thermodynamic properties of the hadron resonance gas computed using the measured hadrons in the particle data book with the correct statistics in the temperature range $T \sim 100$–140 MeV if one imposes an upper cutoff for the mass integrals. In fact, for ρ_1 and ρ_2 the mass cutoff is 1.7 and 1.9 GeV, respectively [26]. We have verified that p/T^4 computed using ρ_3 with a mass cutoff of 1.9 GeV approaches the result obtained using ρ_1 with a mass cutoff of 1.9 GeV. When $T < 100$ MeV, the discreteness of the hadron spectrum becomes relevant and the continuous approximation discussed here gives a poor description of the thermodynamic quantities of a hadron resonance gas. Therefore, to have a hadronic equation of state that is valid at both low temperatures ($T < 100$ MeV) and higher temperatures a hybrid model containing the measured hadron states plus a continuous Hagedorn spectrum above a certain mass cutoff is more appropriate [16–20].

A comparison between $p(T)/T^4$, $(\varepsilon - 3p)/T^4$, and $c_s^2(T)$ of the model defined by Eqs. (4)–(7) (for the four different hadron density of states) and the $N_t = 10$ lattice data of Ref. [15] can be found in Figs. 2–5. The black solid curves denote the result obtained by taking the mass integrals in Eqs. (4)–(7) to infinity while the dashed blue curves were computed imposing an upper mass cutoff that varied for each ρ: For ρ_1 the cutoff is 1.7 GeV, while for ρ_2 and ρ_3 the cutoff is 1.9 GeV. These cutoffs were determined by requiring that the trace anomaly computed in this continuous model matches the result (up to $T \sim 140$ MeV) obtained in a model where all the hadron resonances of the particle data book are included, as defined in Ref. [26].

The power law increase given by ρ_4 considerably simplifies the integrals in Eqs. (4)–(7) and all of them can be done analytically. For instance, one finds in this case that $c_s^2 = 1/(\alpha + 4)$. However, note in Fig. 5 that the power law spectrum lacks the exponential growth necessary to describe the lattice data for temperatures above 140 MeV. This provides evidence that the thermodynamic quantities of QCD computed on the lattice can be understood in terms of a simple hadron resonance gas model with an *exponentially rising* density of states at temperatures $T \sim 100$–155 MeV. This comparison to lattice data cannot pin down the exact subleading power of m in the hadron density of states. However, it is important to note that the specific value of this power has some interesting consequences, as we elaborate below.

The subleading contribution $\sim m^{-a}$ to the density of states at large m, according to Frautschi's seminal paper [27], determines the decay properties of a heavy resonance. For instance, when $a > 5/2$ (which is the case of ρ_3), a heavy resonance decays (in the first generation of its decay chain) into a heavy secondary particle that carries almost all the available mass plus one (with 69% probability) or two light hadrons (with 24% probability). This should be contrasted with Hagedorn's original mass spectrum in Eq. (9) for which

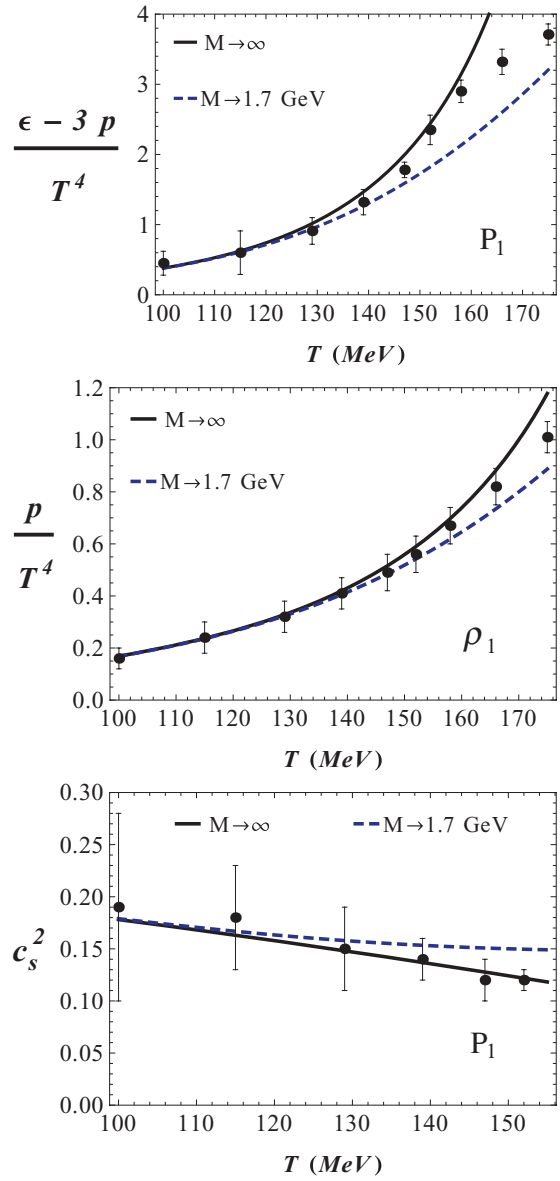

FIG. 2. (Color online) Trace anomaly, pressure, and speed of sound squared for the hadron resonance model with density of states ρ_1. The black solid curves denote the result obtained by taking the mass integrals in Eqs. (4)–(7) to infinity while the dashed blue curves were computed imposing an upper mass cutoff of 1.7 GeV. The data points correspond to the $N_t = 10$ lattice data published in Ref. [15] (obtained from Table 5 in that paper).

the statistically favored process involves a heavy resonance of mass m decaying into a number $n \sim \ln m$ of secondary particles, each of similar mass [27].

It is well known that hadrons interact with each other in a variety of different channels; some of them give rise to repulsive interactions, while others represent attractive interactions. In Ref. [36] the pressure of an interacting gas of pions was calculated within the virial expansion (using experimentally determined phase shifts) and it was shown that the thermodynamic quantities of this interacting system nearly coincides with those of a free gas of pions and ρ

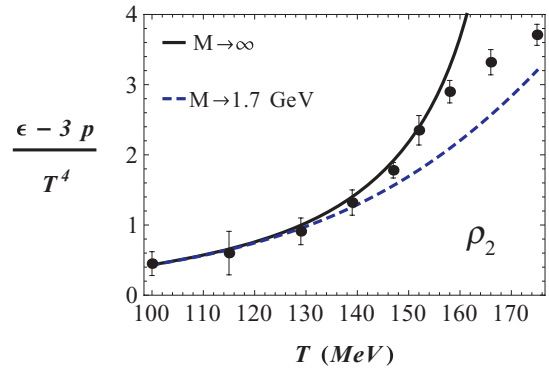

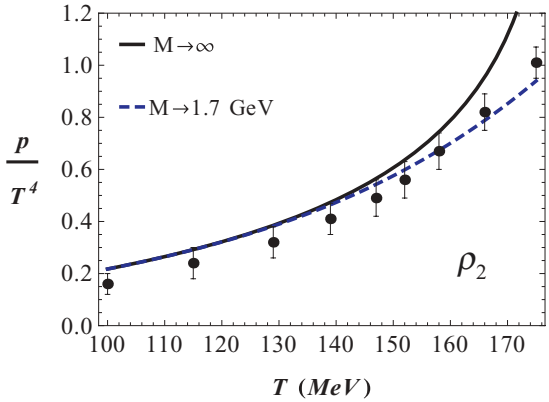

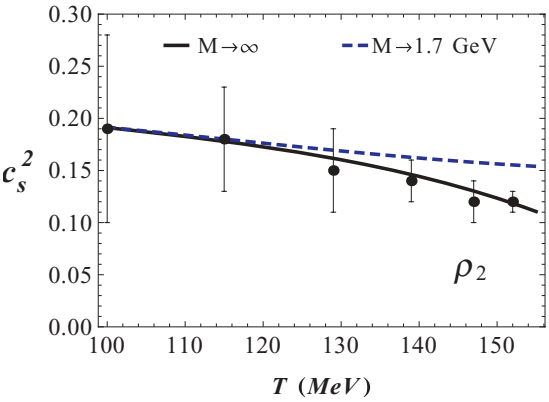

FIG. 3. (Color online) Trace anomaly, pressure, and speed of sound squared for the hadron resonance model with density of states ρ_2. The black solid curves denote the result obtained by taking the mass integrals in Eqs. (4)–(7) to infinity, while the dashed blue curves were computed imposing an upper mass cutoff of 1.9 GeV. The data points correspond to the $N_t = 10$ lattice data published in Ref. [15] (obtained from Table 5 in that paper).

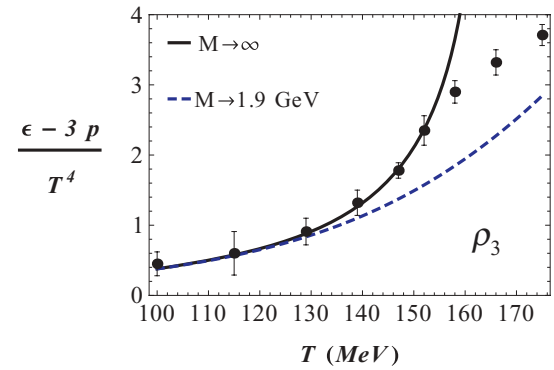

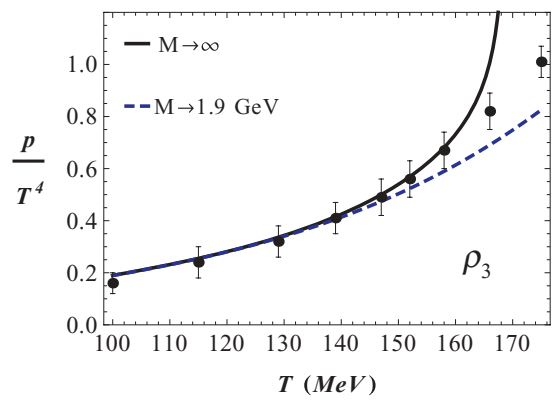

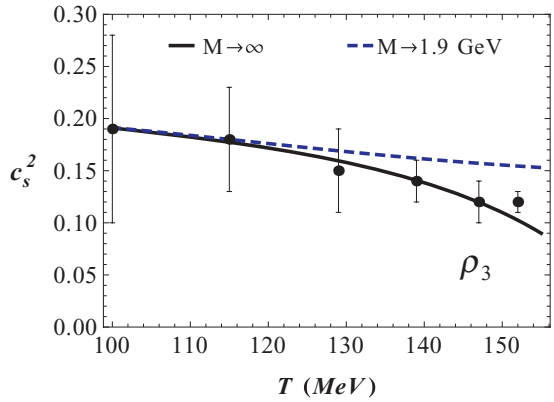

FIG. 4. (Color online) Trace anomaly, pressure, and speed of sound squared for the hadron resonance model with density of states ρ_3. The black solid curves denote the result obtained by taking the mass integrals in Eqs. (4)–(7) to infinity, while the dashed blue curves were computed imposing an upper mass cutoff of 1.9 GeV. The data points correspond to the $N_t = 10$ lattice data published in Ref. [15] (obtained from Table 5 in that paper).

mesons. In this case, there is an approximate cancellation between the attractive and repulsive S-wave channels, which effectively enhances the P-wave contribution from the ρ resonance [37]. As more hadronic species are included, it is not at all guaranteed that the standard assumption behind hadron resonance models, that is, that the interacting hadronic system can be described by a free gas of the original hadrons and their resonances, is applicable. In general, the inclusion of resonances represents the contribution from the attractive channels while repulsive interactions can be modeled using simple excluded volume corrections to the thermodynamics [38–40]. The suggestion, obtained from a comparison to lattice data, that the complicated interactions among hadrons that enter in the calculations of QCD thermodynamics at temperatures of the order of the pion mass can be effectively modeled by a simple, noninteracting gas of hadrons and resonances in accordance with the bootstrap model [21] is therefore quite unexpected and remarkable.

Given the known uncertainties in lattice calculations at low temperatures, the conclusion made above regarding the applicability of the hadron resonance gas should be taken with great care. If results obtained with finer lattices confirm this

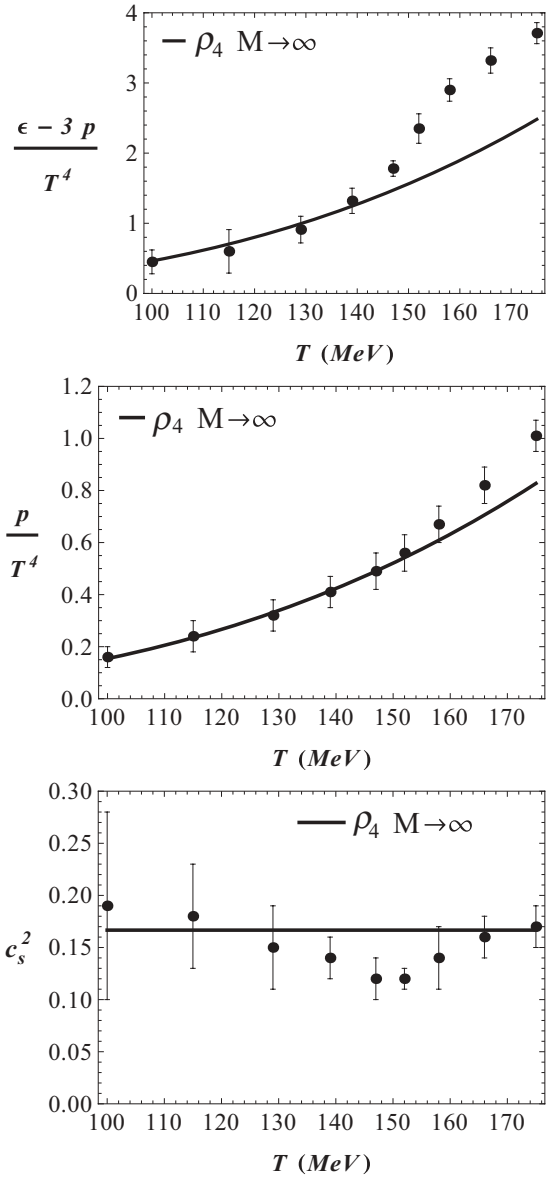

FIG. 5. Trace anomaly, pressure, and speed of sound squared for the hadron resonance model with density of states ρ_4. The black solid curves denote the result obtained by taking the mass integrals in Eqs. (4)–(7) to infinity. The data points correspond to the $N_t = 10$ lattice data published in Ref. [15] (obtained from Table 5 in that paper).

picture, this would provide very strong evidence for the validity of Hagedorn's bootstrap hypothesis. We note in passing that recent lattice calculations of the thermodynamical properties of SU(3) pure glue have shown evidence for the presence of an exponentially rising glueball mass spectrum below the deconfinement critical temperature [41,42].

III. EXCLUDED VOLUME CORRECTIONS TO THE HADRON RESONANCE GAS MODEL

As mentioned in the previous section, in general, one should expect that there are repulsive interactions among hadrons and that a simple way to take that into account in the hadron resonance model is via the excluded volume corrections [38–40]. In this case, the partition function in Eq. (3) becomes

$$Z(T,V) = \sum_{N=0}^{\infty} \frac{1}{N!} \prod_{i=1}^{N} \int dm_i\, \rho(m_i) \times \int \frac{d^3 p_i}{(2\pi)^3} e^{-E_i/T} \left(V - \sum_{j=1}^{N} V_j \right)^N , \qquad (12)$$

where V_j denotes the excluded volume by the jth hadron. We assume for simplicity that the volume excluded by each hadron is a constant that is basically the same for all hadrons, that is, $V_j = v$. This parameter can be written in terms of an effective hard-core volume, $v = 4 \cdot 4\pi r^3/3$, where r is the effective core radius. The excluded volume pressure is determined by the equation

$$\frac{p_v(T)}{T} = n(T) \exp\left(-v p_v(T)/T\right), \qquad (13)$$

where $n(T) = p(T)/T$ is the total particle density computed without volume corrections [40]. The equation above can be solved analytically in terms of the Lambert W function [43] and it reads

$$\frac{p_v(T)}{T} = W(v\, n(T)). \qquad (14)$$

The other thermodynamic quantities, $\varepsilon_v(T)$, $s_v(T)$, and $n_v(T)$, can be obtained through the pressure using the standard thermodynamic identities. In the limit where $v \to 0$ one recovers the formulas in Eqs. (4)–(7).

Given that the free hadronic gas of the previous section provided a good description of the data, one should expect that the volume corrections should be minimal in this case. In fact, one can again use the lattice data and the different hadron mass spectra discussed before to show that the excluded radius cannot be larger than 0.2 fm for ρ_i $(i = 1, 2, 3)$. ρ_4 is not considered in this case because it fails to describe the data for $T > 140$ MeV. We show a comparison between the lattice data and the ρ_3 model curves for $r = 0.2$ fm in Fig. 6. The small excluded volume shifts the curves slightly downwards, which makes them get closer to the lattice data at $T = 160$ MeV. Similar results hold for the other exponentially increasing spectra considered before. For larger excluded volumes the hadron resonance gas curves start to deviate from the lattice at lower temperatures and this is why we here take $r \leqslant 0.2$ fm. This analysis shows that volume corrections do not play a significant role in the description of lattice data (at least for the mass spectra parameters determined in the previous section). Of course, given the known uncertainties in lattice calculations at low temperatures, another possibility would be to define the parameters in a way that the model including the continuous spectrum fits the lattice data only at higher temperatures around $T \sim 150$ MeV, as was done in Ref. [17]. This is discussed further in the next section.

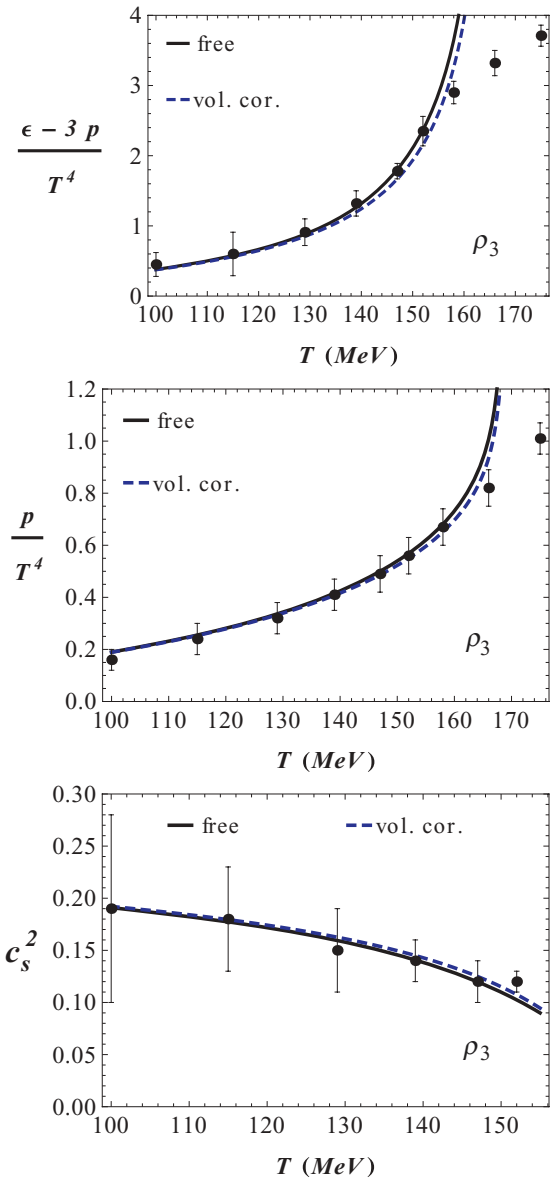

FIG. 6. (Color online) Trace anomaly, pressure, and speed of sound squared for the hadron resonance model with density of states ρ_3 and an excluded volume radius of $r = 0.2$ fm. The dashed blue curves denote the excluded volume results, while the solid black curves show the corresponding quantities without excluded volume corrections. The data points correspond to the $N_t = 10$ lattice data published in Ref. [15] (obtained from Table 5 in that paper).

IV. CALCULATION OF THE SHEAR VISCOSITY TO ENTROPY DENSITY RATIO AND THE SHEAR RELAXATION TIME COEFFICIENT OF THE HADRON RESONANCE GAS MODEL WITH EXCLUDED VOLUME CORRECTIONS

The computation of the transport properties of a hadronic mixture is not an easy task. There have been several studies on this subject in the last few years [9–12,17,44,45]. To find at least an estimate of the order of magnitude of the η/s ratio of hot hadronic matter at $T \sim 160$ MeV, we follow the approximations made by Ref. [9], where the shear viscosity of a multicomponent gas of hadrons and resonances in the excluded volume approximation (described in the previous section) is given by

$$\eta = \frac{5}{64\, r^2}\left(\frac{T}{\pi}\right)^{1/2} \frac{T}{2\pi^2\, n(T)} \int_0^\infty dm\, \rho(m)\, m^{5/2} K_{5/2}\left(\frac{m}{T}\right). \tag{15}$$

Currently, it is not known how to compute the contribution to the shear viscosity from heavily massive and highly unstable resonances that cannot rigorously be described using the Boltzmann equation. These states contribute significantly to the thermodynamic properties of the matter at high temperatures (as shown in the previous sections) and, owing to their rapid decay, it is natural to assume that their presence will affect the mean free paths of the other hadrons. In Ref. [17], it was assumed that the mean free path of these resonances with $m > 2$ GeV equals their inverse decay width. Obviously, further studies have to be carried out to properly include the effects of Hagedorn states on transport coefficients of hot hadronic matter. While the formula in Eq. (15) may only provide an estimate of the shear viscosity of an interacting hadron gas, the temperature behavior of η computed with this approximation [9] follows the estimates made using other methods and thus we proceed using this formula.

In Eq. (15), the dependence on the excluded radius only appears via the $1/r^2$ factor. However, when computing η/s, the entropy density should be the one determined within the same approximation, that is, $s_v(T)$. Therefore, even in this approximation η/s possesses a nontrivial dependence on the hadron cross section $\sim r^2$. This is shown in Fig. 7, where the η/s ratio is computed for different r's using ρ_3 (10) and $T = 155$ MeV. Note that for the highest temperature considered, $T = 155$ MeV, η/s depends very weakly on r

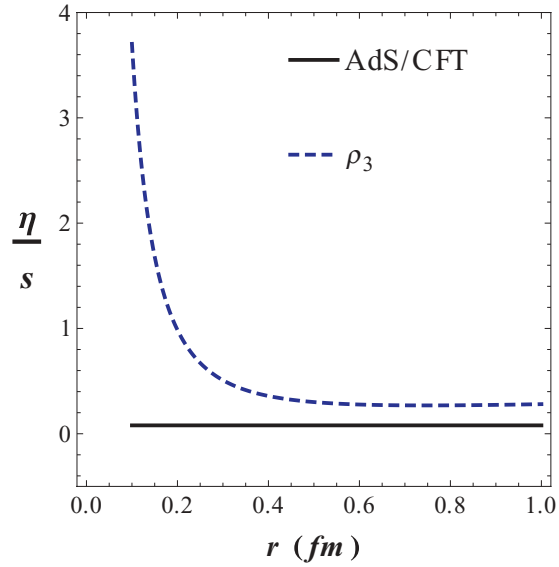

FIG. 7. (Color online) The ratio η/s (dashed blue line) as a function of the excluded volume radius computed via (15) using the density of states ρ_3 in Eq. (10) and $T = 155$ MeV. The black line denotes the viscosity lower bound $\eta/s = 1/(4\pi)$.

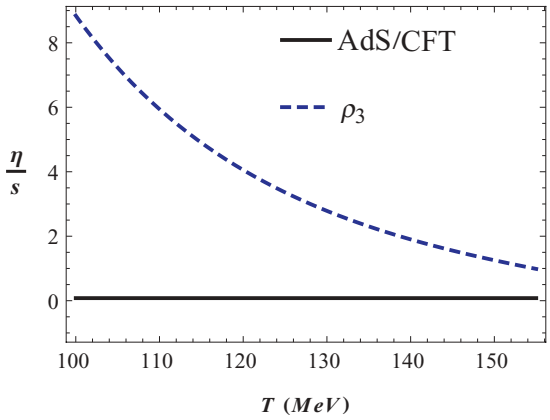

FIG. 8. (Color online) The ratio η/s (dashed blue line) computed within the excluded volume approximation defined via Eqs. (13) and (15) using the density of states ρ_3 in Eq. (10) and $r = 0.2$ fm. The entropy density computed in this model fits the lattice data [15] in the temperature range shown. The black line denotes the viscosity lower bound $\eta/s = 1/(4\pi)$.

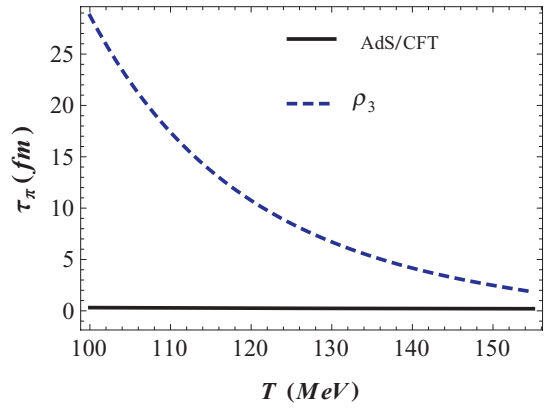

FIG. 9. (Color online) The lowest relaxation time coefficient τ_π computed using the inequality in Eq. (16) for the hadron resonance gas model defined with density of states ρ_3 and η/s and c_s^2 computed within the excluded volume approximation with excluded volume radius $r = 0.2$ fm (dashed blue curve). The black line denotes the lowest value for τ_π in a conformal "nearly perfect" fluid, where $c_s^2 = 1/3$ and $\eta/s = 1/(4\pi)$.

when the excluded radius is larger than 0.2 fm (using this specific set of parameters that define the mass spectrum).

In Fig. 8 we show the temperature dependence of η/s computed using the density of states ρ_3 in Eq. (10) and $r = 0.2$ fm. As discussed in the previous section, for the specific choice of parameters that define ρ_3, calculations of thermodynamical quantities performed with an excluded radius of $r = 0.2$ fm can describe the lattice data in the entire temperature range, $T = 100$–160 MeV. This value of the excluded radius is smaller than other estimates [9], which, however, were not constrained by fitting the lattice data. Perhaps it would be more physical to consider a model where the excluded radius increases with the mass of the hadron but for simplicity's sake in the current study we limit ourselves to a constant excluded radius, hoping that we are correct within an order of magnitude. In Fig. 8, we see that the η/s ratio remains an order of magnitude above the viscosity lower bound up to $T = 155$ MeV (this remains the case when other expressions for the density of states mentioned in the previous sections are used). The entropy density computed in this case matches the lattice data well, as it can be inferred from the other quantities shown in Fig. 6. Therefore, this simple hadron resonance gas model with constant excluded volume corrections is able to describe the thermodynamic quantities computed by lattice data below $T = 160$ MeV and the corresponding η is computed self-consistently within the same framework.

In viscous hydrodynamic calculations of the QGP time evolution [1–3], there is at least another transport coefficient that must be included in the fluid equations, the shear viscosity relaxation time τ_π, which enters in second-order viscous hydrodynamic calculations. In fact, in relativistic fluids causality is intimately connected to stability [46,47] and Israel and Stewart [48] were among the first to understand that the characteristic times within which fluid dynamical dissipative currents relax towards their asymptotic Navier-Stokes values cannot be arbitrarily small. Using the Boltzmann equation, it is possible to show [48–51] that in relativistic gases τ_π is of the order of the microscopic collision time. A detailed linear stability analysis made in Ref. [52] showed that stability and causality require that τ_π in any viscous relativistic fluid cannot be arbitrarily small. In fact, this transport coefficient must obey the following inequality [52]:

$$\tau_\pi \geqslant \frac{4}{3}\frac{\eta}{s\,T}\frac{1}{\left(1-c_s^2\right)}. \tag{16}$$

While we do not compute τ_π for the hadron resonance gas model considered here, we find it instructive to consider the smallest τ_π implied by the inequality above because it provides an estimate for the value of this parameter that can be used in hydrodynamic simulations. In Fig. 9 we show (dashed blue line) the lowest value for τ_π computed using the η/s in Fig. 8 that fulfills the stability and causality criteria. We

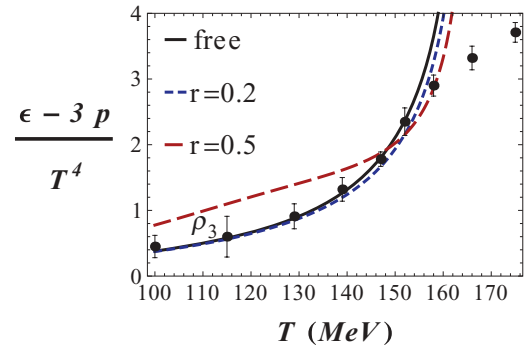

FIG. 10. (Color online) Comparison between the model's trace anomaly computed different excluded volumes and the $N_t = 10$ lattice data published in Ref. [15] (obtained from Table 5 in that paper). The solid black curve was computed using ρ_3 with the parameters defined in Table I. The short-dashed blue curve is computed using the same ρ_3 but with an excluded volume of $r = 0.2$ fm. The long-dashed red curve was computed using ρ_3 but with $A_3 = 3.7$ GeV^2 and $m_{03} = 1$ GeV together with an excluded volume of $r = 0.5$ fm.

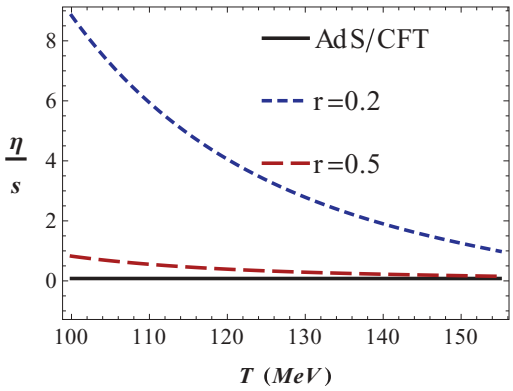

FIG. 11. (Color online) The ratio η/s computed within the excluded volume approximation. The short-dashed blue curve is computed using ρ_3 with the parameters defined in the Table I but with an excluded volume of $r = 0.2$ fm. The long-dashed red curve was computed using ρ_3 but with $A_3 = 3.7$ GeV^2 and $m_{03} = 1$ GeV together with an excluded volume of $r = 0.5$ fm.

also show in the same plot the lowest value for τ_π in a generic conformal "nearly perfect" fluid where $c_s^2 = 1/3$ and $\eta/s = 1/(4\pi)$ for reference. Note that the lowest value of τ_π computed in the hadron resonance gas model employed here remains well above the lowest value for a nearly perfect fluid up to $T = 160$ MeV.

Throughout our calculations thus far we have the underlying assumption that the hadron gas model must fit the entire lower temperature region $T \sim 100$ MeV of the lattice data. However, it is interesting to consider the possibility of just fitting the lattice data at higher temperatures $T \sim 150$ MeV to see how that affects the η/s calculation. This can be accomplished by changing some of the parameters of the hadron mass spectrum. Before doing so, we increase $r = 0.5$ fm [9]. Then we refitted the parameters A_3 and m_{03} in Eq. (10) to fit only the high-temperature region of the lattice trace anomaly. This is shown in Fig. 10. The corresponding η/s and shear relaxation time

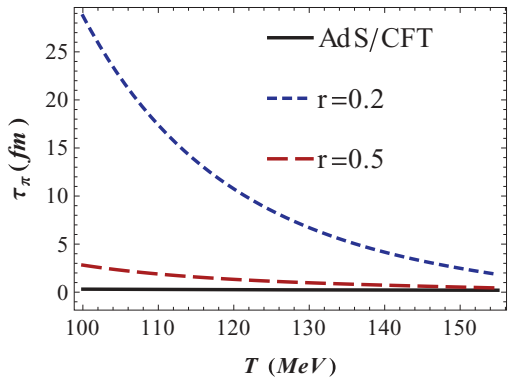

FIG. 12. (Color online) The lowest relaxation time coefficient τ_π computed using the inequality in Eq. (16) for the hadron resonance gas model. The short-dashed blue curve is computed using ρ_3 with the parameters defined in the Table I but with an excluded volume of $r = 0.2$ fm. The long-dashed red curve was computed using ρ_3 but with $A_3 = 3.7$ GeV^2 and $m_{03} = 1$ GeV together with an excluded volume of $r = 0.5$ fm.

computed with this setup are shown in Figs. 11 and 12. Note that with this new set of parameters η/s drops down to $1/(4\pi)$ around $T = 160$ MeV and τ_π also decreases significantly in that region. The decrease of the transport coefficients is mainly driven by the larger entropy that results from this new fit that is only constrained by the higher lattice temperatures. This emphasizes the sensitivity of such calculations to the thermodynamic properties of the matter.

V. CONCLUSIONS

In this paper we performed a detailed comparison of hadron resonance gas model calculations to recent lattice data [15] that confirmed the need for an exponentially increasing density of hadronic states. Also, we showed that the hadron mass spectrum, extracted from a comparison to lattice data, is compatible with $\rho(m) \sim m^{-a} \exp(m/T_H)$ at large m with $a > 5/2$ (where $T_H \sim 167$ MeV). With this specific m^{-a} (with $a > 5/2$) factor in the density of states, heavy resonances most likely undergo two-body decay (instead of multiparticle decay) [27], which facilitates their inclusion into hadron transport codes. Moreover, we have computed the shear viscosity to entropy density ratio of this system within the excluded volume approximation and the results suggest that η/s of hot hadronic matter is very sensitive to the temperature dependence of the thermodynamic quantities. Using this calculation of η/s, we were able to compute the lowest value for the shear relaxation time coefficient used in second-order hydrodynamic calculations that respects the criteria of causality and stability of a relativistic viscous fluid.

Previous estimates for the η/s ratio in a hadronic gas [17] had concluded that hadronic matter at temperatures $T \sim 190$ MeV behaved as a nearly perfect fluid. This is not at odds with the findings presented in this paper as we explained in the previous section. In fact, the curve shown in Fig. 8 approaches $1/(4\pi)$ when continued to temperatures $\sim$190 MeV. Moreover, if only the high-temperature region of the lattice data is fitted, then the transport coefficients calculated here decrease significantly [e.g., $\eta/s \sim 1/(4\pi)$ near $T = 160$ MeV]. This highlights the importance of knowing the correct temperature dependence of the thermodynamic quantities of QCD at temperatures $\sim$100–160 MeV because it may play an important role in the calculation of transport coefficients.

The key difference between these studies is the lattice data used as a reference for the hadron gas calculations. Reference [17] used the most recent lattice data at the time [22], which indicated a phase transition pseudocritical temperature $T_c \sim 196$ MeV. The much lower value for this pseudocritical temperature found in Refs. [15,24] severely reduced the value of the maximum temperature at which the hadron resonance gas is still applicable because "T_c" decreased from 190 to 160 MeV. Given that this low pseudocritical temperature has already been independently confirmed by other lattice groups [25], if there is no change in the low-temperature behavior of the thermodynamic quantities as determined by lattice, the analysis performed in this paper indicates that the hot hadronic matter formed in ultrarelativistic heavy-ion collisions is far from being a nearly perfect fluid. However, this should be

taken with a grain of salt given the sensitivity mentioned above within the transport coefficients.

Because $(\varepsilon - 3p)/T^4$ in the lattice data [15] continues to increase until it reaches a turning point around $T \sim 200$ MeV, one may wonder if it is possible to devise a model that reduces to the Hagedorn resonance gas discussed here at low temperatures that also incorporates the correct degrees of freedom in the crossover region between $T \sim 160$ MeV and $T \sim 200$ MeV [53]. Perhaps such an effective model can be constructed by taking into account the Polyakov loop [54].

ACKNOWLEDGMENTS

This work was partially supported by the Helmholtz International Center for FAIR within the framework of the LOEWE program launched by the State of Hesse. J. Noronha-Hostler is supported by Fundacao de Amparo a Pesquisa do Estado de Sao Paulo (FAPESP). J. Noronha thanks Conselho Nacional de Desenvolvimento Cientifico e Tecnologico (CNPq) and Fundacao de Amparo a Pesquisa do Estado de Sao Paulo (FAPESP) for financial support.

[1] B. Schenke, S. Jeon, and C. Gale, Phys. Rev. Lett. **106**, 042301 (2011); Phys. Rev. C **85**, 024901 (2012).
[2] H. Song, S. A. Bass, and U. Heinz, Phys. Rev. C **83**, 054912 (2011); H. Song, S. A. Bass, U. Heinz, T. Hirano, and C. Shen, *ibid*. **83**, 054910 (2011); Phys. Rev. Lett. **106**, 192301 (2011).
[3] P. Romatschke and U. Romatschke, Phys. Rev. Lett. **99**, 172301 (2007); M. Luzum and P. Romatschke, Phys. Rev. C **78**, 034915 (2008); **79**, 039903(E) (2009); K. Dusling and D. Teaney, *ibid*. **77**, 034905 (2008); H. Niemi, G. S. Denicol, P. Huovinen, E. Molnar, and D. H. Rischke, Phys. Rev. Lett. **106**, 212302 (2011).
[4] P. Danielewicz and M. Gyulassy, Phys. Rev. D **31**, 53 (1985).
[5] A. Buchel and J. T. Liu, Phys. Rev. Lett. **93**, 090602 (2004); P. K. Kovtun, D. T. Son, and A. O. Starinets, *ibid*. **94**, 111601 (2005).
[6] J. M. Maldacena, Adv. Theor. Math. Phys. **2**, 231 (1998); S. S. Gubser, I. R. Klebanov, and A. M. Polyakov, Phys. Lett. B **428**, 105 (1998); E. Witten, Adv. Theor. Math. Phys. **2**, 253 (1998).
[7] P. B. Arnold, G. D. Moore, and L. G. Yaffe, J. High Energy Phys. 11 (2000) 001; 05 (2003) 051.
[8] Z. Xu and C. Greiner, Phys. Rev. Lett. **100**, 172301 (2008); Z. Xu, C. Greiner, and H. Stocker, *ibid*. **101**, 082302 (2008); A. El, A. Muronga, Z. Xu, and C. Greiner, Phys. Rev. C **79**, 044914 (2009); C. Wesp, A. El, F. Reining, Z. Xu, I. Bouras, and C. Greiner, *ibid*. **84**, 054911 (2011); J. Fuini, III, N. S. Demir, D. K. Srivastava, and S. A. Bass, J. Phys. G **38**, 015004 (2011).
[9] M. I. Gorenstein, M. Hauer, and O. N. Moroz, Phys. Rev. C **77**, 024911 (2008).
[10] K. Itakura, O. Morimatsu, and H. Otomo, Phys. Rev. D **77**, 014014 (2008).
[11] N. Demir and S. A. Bass, Phys. Rev. Lett. **102**, 172302 (2009).
[12] S. Pal, Phys. Lett. B **684**, 211 (2010).
[13] L. P. Csernai, J. I. Kapusta, and L. D. McLerran, Phys. Rev. Lett. **97**, 152303 (2006); T. Hirano and M. Gyulassy, Nucl. Phys. A **769**, 71 (2006).
[14] M. Cheng, S. Ejiri, P. Hegde, F. Karsch, O. Kaczmarek, E. Laermann, R. D. Mawhinney, C. Miao *et al*., Phys. Rev. D **81**, 054504 (2010).
[15] S. Borsanyi, G. Endrodi, Z. Fodor, A. Jakovac, S. D. Katz, S. Krieg, C. Ratti, and K. K. Szabo, J. High Energy Phys. 11 (2010) 077.
[16] J. Noronha-Hostler, C. Greiner, and I. A. Shovkovy, Phys. Rev. Lett. **100**, 252301 (2008).
[17] J. Noronha-Hostler, J. Noronha, and C. Greiner, Phys. Rev. Lett. **103**, 172302 (2009).
[18] J. Noronha-Hostler, H. Ahmad, J. Noronha, and C. Greiner, Phys. Rev. C **82**, 024913 (2010).
[19] J. Noronha-Hostler, J. Noronha, H. Ahmad, I. Shovkovy, and C. Greiner, Nucl. Phys. A **830**, 745C (2009).
[20] J. Noronha-Hostler, M. Beitel, C. Greiner, and I. Shovkovy, Phys. Rev. C **81**, 054909 (2010).
[21] R. Hagedorn, Nuovo Cim. Suppl. **3**, 147 (1965); Nuovo Cim. A **56**, 1027 (1968).
[22] M. Cheng, N. H. Christ, S. Datta, J. van der Heide, C. Jung, F. Karsch, O. Kaczmarek, E. Laermann *et al*., Phys. Rev. D **77**, 014511 (2008).
[23] T. Schafer and D. Teaney, Rept. Prog. Phys. **72**, 126001 (2009).
[24] Y. Aoki, Z. Fodor, S. D. Katz, and K. K. Szabo, Phys. Lett. B **643**, 46 (2006); Y. Aoki, S. Borsanyi, S. Durr, Z. Fodor, S. D. Katz, S. Krieg, and K. K. Szabo, J. High Energy Phys. 06 (2009) 088; S. Borsanyi *et al*. (Wuppertal-Budapest Collaboration), *ibid*. 09 (2010) 073.
[25] A. Bazavov, T. Bhattacharya, M. Cheng, C. DeTar, H. T. Ding, S. Gottlieb, R. Gupta and P. Hegde *et al*., Phys. Rev. D **85**, 054503 (2012).
[26] A. Majumder and B. Muller, Phys. Rev. Lett. **105**, 252002 (2010).
[27] S. C. Frautschi, Phys. Rev. D **3**, 2821 (1971).
[28] S. Fubini and G. Veneziano, Nuovo Cimento **64A**, 811 (1969); K. Bardakgi and S. Mandelstam, Phys. Rev. **184**, 1640 (1969); S. Fubini, D. Gordon, and G. Veneziano, Phys. Lett. B **29**, 679 (1969).
[29] K. Huang and S. Weinberg, Phys. Rev. Lett. **25**, 895 (1970).
[30] T. D. Cohen, Phys. Lett. B **637**, 81 (2006).
[31] C. B. Thorn, Phys. Lett. B **99**, 458 (1981).
[32] S. Eidelman *et al*., Phys. Lett. B **592**, 1 (2004).
[33] W. Broniowski and W. Florkowski, Phys. Lett. B **490**, 223 (2000).
[34] W. Broniowski, W. Florkowski, and L. Y. Glozman, Phys. Rev. D **70**, 117503 (2004).
[35] E. V. Shuryak, Yad. Fiz. **16**, 395 (1972).
[36] G. M. Welke, R. Venugopalan, and M. Prakash, Phys. Lett. B **245**, 137 (1990).
[37] R. Venugopalan and M. Prakash, Nucl. Phys. A **546**, 718 (1992).
[38] R. Hagedorn and J. Rafelski, Phys. Lett. B **97**, 136 (1980).
[39] J. I. Kapusta and K. A. Olive, Nucl. Phys. A **408**, 478 (1983).
[40] D. H. Rischke, M. I. Gorenstein, H. Stoecker, and W. Greiner, Z. Phys. C **51**, 485 (1991).
[41] H. B. Meyer, Phys. Rev. D **80**, 051502 (2009).

[42] S. Borsanyi, G. Endrodi, Z. Fodor, S. D. Katz, and K. K. Szabo, arXiv:1204.6184 [hep-lat].

[43] The Lambert $W(z)$ function is the solution of the differential equation $dW(z)/dz = W(z)/[z(1 + W(z))]$ (for $z \neq 0$) as discussed in http://mathworld.wolfram.com/LambertW-Function.html.

[44] M. Prakash, M. Prakash, R. Venugopalan, and G. M. Welke, Phys. Rev. Lett. **70**, 1228 (1993); Phys. Rep. **227**, 321 (1993).

[45] P. Chakraborty and J. I. Kapusta, Phys. Rev. C **83**, 014906 (2011).

[46] W. A. Hiscock and L. Lindblom, Ann. Phys. (NY) **151**, 466 (1983); Phys. Rev. D **31**, 725 (1985); **35**, 3723 (1987); Phys. Lett. A **131**, 509 (1988); **131**, 509 (1988).

[47] G. S. Denicol, T. Kodama, T. Koide, and Ph. Mota, J. Phys. G **35**, 115102 (2008); S. Pu, T. Koide, and D. H. Rischke, Phys. Rev. D **81**, 114039 (2010).

[48] W. Israel and J. M. Stewart, Phys. Lett. A **58**, 213 (1976); Ann. Phys. (NY) **118**, 341 (1979); Proc. R. Soc. London, Ser. A **365**, 43 (1979).

[49] G. S. Denicol, T. Koide, and D. H. Rischke, Phys. Rev. Lett. **105**, 162501 (2010).

[50] G. S. Denicol, H. Niemi, E. Molnar, and D. H. Rischke, arXiv:1202.4551 [nucl-th].

[51] G. S. Denicol, J. Noronha, H. Niemi, and D. H. Rischke, Phys. Rev. D **83**, 074019 (2011).

[52] S. Pu, T. Koide, and D. H. Rischke, Phys. Rev. D **81**, 114039 (2010).

[53] Y. Aoki, G. Endrodi, Z. Fodor, S. D. Katz, and K. K. Szabo, Nature (London) **443**, 675 (2006).

[54] A. Dumitru, Y. Guo, Y. Hidaka, Christiaan P. Korthals Altes, and R. D. Pisarski, Phys. Rev. D **83**, 034022 (2011).